DEVELOPMENT OF NONSYNCHRONOUS MODES IN COUPLED SYSTEMS WITH PHASE AND DELAY CONTROL

Valery P. Ponomarenko

Research Institute of Applied Mathematics and Cybernetics,
Nizhni Novgorod, Russia, povp@uic.nnov.ru

Abstract

Dynamical modes, bifurcations and chaotic behavior of two coupled phase-lock and delay-lock systems are investigated. One of the interacting systems demonstrates only regular modes while the other system exhibits both regular and chaotic modes. Numerical simulations of corresponding nonlinear five-dimensional dynamical model reveal various periodic and chaotic oscillatory modes. The stability conditions of synchronous regime are determined, dynamical behavior of the system under variation initial frequency mistuning is shown. The results are present in the form of one-parameter bifurcation diagrams and phase portraits of the system attractors.

Key words

Phase-lock and delay-lock systems, regular and chaotic modes, synchronous regime, bifurcations and chaotic behavior, phase space, attractors, bifurcation diagrams, phase portraits.

1 Introduction

At present, phenomena of complex dynamics in coupled auto-oscillating systems arouse heightened interest with researchers. Coupled oscillatory systems with phase and delay control are considered as interesting objects, in which variation of the control circuits parameters enables one to implement efficient influence on the properties and regions of existence of generated oscillations. In this paper we investigate various types of dynamical modes observed from double-loop tracking system (DLTS) consisting of mutually coupled phase-locked loop (PLL) and delay-locked loop (DLL).

DLTS are widely utilized in many communication technology and radio navigation for solving problem of the simultaneous tracking estimation of parameters of a wideband pseudo-random signal (phase angle $\vartheta(t)$ and time delay $T(t)$) [Tuzov, Sivov, Prytkov, et al.,1985] and [Babich, 1991]. The DLTS dynamics, when out-of-lock, is essentially nonlinear with periodic nonlinearity. The following stationary regimes may be realized:

a regime of synchronization, when phase $\varphi=\vartheta(t)-\vartheta^*(t)$ and delay $\eta=T(t)-T^*(t)$ errors attain minimum values ($\vartheta^*(t)$ and $T^*(t)$ are parameters of reference signal, i.e. the estimations of parameters $\vartheta(t)$ and $T(t)$);

a quasi-synchronous mode, in which the system exhibits self-modulation oscillations about synchronous regime that becomes unstable;

an asynchronous mode with rotation of phase difference φ.

We focus our attention to the dynamical modes and bifurcation transitions occurring in the model of DLTS in the case when the PLL subsystem autonomously exhibits only regular behavior, whereas an isolated DLL system may operate in both regular and chaotic oscillation modes. By carrying out computer simulation, we confirmed that various kind of dynamical states from simple periodic regimes to chaotic ones were observed in DLTS under study. The study of emergence and development of nonsynchronous modes, as well as revealing the role of the control circuit parameters and coupling between partial systems PLL and DLL, have both theoretical and applied importance.

2 The dynamical model under consideration

The mathematical model of considered DLTS can be represent in the following operator form *($p\equiv d/dt$)* [Ponomarenko, 2002]

$$\begin{aligned} &p\varphi / k + K_1(p)R(x)\sin\varphi = \gamma, \\ &x + bK_2(p)(D(x) + \alpha b^{-1}R(x)\sin\varphi) = \sigma, \end{aligned} \tag{1}$$

where φ and x are phase and delay errors, γ and σ are the relative initial frequency and delay mistuning, k and b represent the control circuits gains, α is a parameter of coupling through mismatch signals, $K_1(p)$ and $K_2(p)$ are the transfer functions of filters in feedback loops, $R(x)$ is autocorrelation function of pseudo-random signal, functions $\sin\varphi$ and $D(x)$ are the characteristics of discriminators in PLL and DLL, respectively. Characteristics $R(x)$ and $\cos\varphi$ may be interpreted as coupling nonlinearities. We consider nonperiodic piecewise-linear characteristics $R(x)$ and $D(x)$ having the form

$$R(x)=\begin{cases} 1+x, & -1\le x\le 0,\\ 1-x, & 0\le x\le 1,\\ 0, & |x|\ge 1,\end{cases}\quad D(x)=\begin{cases} -2-x, & -2\le x\le -1,\\ x, & -1\le x\le 1,\\ 2-x, & 1\le x\le 2,\\ 0, & |x|\ge 2.\end{cases}$$

According to the formulation of the problem, we set in equations (1) $K_1(p)=(1+mT_1p)/(1+T_1p)$, $K_2(p)=1/(1+$ $+(T_2+T_3+T_4)p+(T_2T_3+T_2T_4+T_3T_4)p^2+T_2T_3T_4p^3)$, where T_1, T_2, T_3, and T_4 are the inertia parameters, $0<m<1$. The equations that correspond to such filters and describe the dynamics of processes in the DLTS under study have the form [Ponomarenko, 2002]

$$\begin{aligned} \frac{d\varphi}{d\tau} &= u - mR(x)\sin\varphi,\\ \varepsilon_1\frac{du}{d\tau} &= \gamma - u - (1-m)R(x)\sin\varphi,\\ \frac{dx}{d\tau} &= y,\\ \frac{dy}{dz} &= z,\\ \varepsilon_2\varepsilon_3\varepsilon_4\frac{dy}{d\tau} &= \sigma - x - bD(x) - (\varepsilon_2+\varepsilon_3+\varepsilon_4)y - \\ &\quad -(\varepsilon_2\varepsilon_3+\varepsilon_2\varepsilon_4+\varepsilon_3\varepsilon_4)z - \alpha R(x)\sin\varphi. \end{aligned} \qquad (2)$$

In equations (2), τ is dimensionless time; $\varepsilon_i=kT_i$ (i=1,2, 3,4). System (2) is defined in the cylindrical phase spaces $U=((\varphi(mod\ 2\pi), u, x, y, z)$ with the space of parameters $\Lambda=\{\gamma,\sigma,\varepsilon_1,\varepsilon_2,\varepsilon_3,\varepsilon_4,\alpha,b,m\}$.

3 Synchronous mode stability

The equilibrium states of system (2) are determinate from the equations

$$\gamma-R(x)\sin\varphi=0,\ \sigma-\alpha\gamma-x-bD(x)=0,$$
$$u=m\gamma,\ y=0,\ z=0.$$

An analysis of these equations shows that system (2) has two equilibrium states $A_1(\varphi_1,m\gamma,x_1,0,0)$ and $A_2(\pi-\varphi_1,m\gamma,x_1,0,0)$ for the parameters from region $C_0=\{max(\gamma_3,\gamma_4)<\gamma<min(\gamma_1,\gamma_2)\}$, where

$$\gamma_1=(1+b-\sigma)/(1+b-\alpha),\ \gamma_2=(1+b+\sigma)/(1+b+\alpha),$$
$$\gamma_3=-(1+b+\sigma)/(1+b-\alpha),\ \gamma_4=-(1+b-\sigma)/(1+b+\alpha).$$

The coordinates φ_1 and x_1 are defined by

$$\varphi_1=arcsin(\gamma/(1-x_1\cdot sign(\sigma-\alpha\gamma))),\ x_1=(\sigma-\alpha\gamma)/(1+b).$$

By investigating the roots of the characteristic equation for the eigenvalues of the linearized system near the equilibrium states

$$\lambda^5+q_1\lambda^4+q_2\lambda^3+q_3\lambda^2+q_4\lambda+q_0=0, \qquad (3)$$

where

$$q_1=-(a_1+b_1+c_1),\ q_2=b_1(a_1+c_1)+a_1c_1-b_2-c_2,$$
$$q_3=-(a_1b_1c_1-(a_1+b_1)c_2+c_3-b_2c_1),$$
$$q_4=-(c_2(a_1b_1-b_2)+a_2c_4-c_3(a_1+b_1)),$$
$$q_0=c_4(a_2b_1-b_3)+c_3(b_2-a_1b_1),$$
$$a_1=-\mathrm{m}((1-(\sigma-\alpha\gamma)\cdot \mathrm{sign}(\sigma-\alpha\gamma)/(1+\mathrm{b}))^2-\gamma^2)^{1/2},$$
$$a_2=\mathrm{m}\gamma\cdot \mathrm{sign}(\sigma-\alpha\gamma)/(1-(\sigma-\alpha\gamma)\cdot \mathrm{sign}(\sigma-\alpha\gamma)/(1+\mathrm{b})),$$
$$b_1=-1/\varepsilon_1,\ b_2=(1-\mathrm{m})a_1(\mathrm{m}\varepsilon_1)^{-1},$$
$$c_1=-(\varepsilon_2\varepsilon_3+\varepsilon_2\varepsilon_4+\varepsilon_3\varepsilon_4)(\varepsilon_2\varepsilon_3\varepsilon_4)^{-1},$$
$$c_2=-(\varepsilon_2+\varepsilon_3+\varepsilon_4)(\varepsilon_2\varepsilon_3\varepsilon_4)^{-1},$$
$$c_3=(\alpha a_2-\mathrm{m}(1+\mathrm{b}))(\mathrm{m}\varepsilon_2\varepsilon_3\varepsilon_4)^{-1},\ c_4=\alpha a_1(\mathrm{m}\varepsilon_2\varepsilon_3\varepsilon_4)^{-1},$$

we find that the equilibrium state A_1 are stable when the following conditions are satisfied

$$q_1, q_2, q_3, q_4, q_0>0,\ q_1q_2-q_3>0,$$
$$(q_1q_2-q_3)(q_3q_4-q_2q_0)-(q_1q_4-q_0)^2>0 \qquad (4)$$

whereas the equilibrium state A_2 is unstable.

The stable equilibrium state A_1 correspond to the regime of synchronization which may be realized in the DLTS if conditions (4) are fulfilled. In the task of tracking estimation of incoming signal's parameters ϑ and T regime of synchronization is a main operational state of DLTS. Values φ_1 and x_1 characterize the accuracy with which parameters ϑ and T are estimated.

4 The system dynamics under variation of initial frequency mistuning

The dynamical states and bifurcations of model (2) for the parameters values outside the region C_s when equilibrium state A_1 is unstable have been studied by a numerical simulation with the help of qualitative-numerical methods of analysis of nonlinear dynamic systems. Numerical simulation shows that a large number of limit cycles of oscillatory and rotatory types may exist in the phase space U [Ponomarenko, 2002].

Let us consider the system's behavior when the boundary of region C_s is crossed owing to variation in parameters of model (2). In this case conditions (4) are violated and system (2) exhibit Andronov-Hopf bifurcation, when characteristic equation (3) has two complex-conjugated roots with a positive real-valued part. This bifurcation gradually induces in the phase space U oscillatory type limit cycle S_0 where phase difference φ varies within a limited range not exceeding 2π. Fig.1a shows (φ,x)-projection of the phase portrait of cycle S_0. Cycle S_0 corresponds to a quasi-synchronous mode of DLTS where periodic oscillations of phase variables are observed around equilibrium state A_1.

As γ increases, limit cycle S_0 disappears as a result of a saddle-node bifurcation. Intermittency accompanies this bifurcation – the long regular stage of the oscillation process alternates with relatively short irregular splashes of rotatory motions. Chaotic attractor P_0 of oscillatory-rotatory type emerges in the phase space as a result of alternation. The corresponding (φ,x)- and (u,x)-projection of the phase portrait and realization $\varphi(\tau)$ and $u(\tau)$ are shown in Figs.1*b*-1*e*. As γ increases, the time of the stage of the oscillatory motions decreases, while the frequency and duration of rotatory motions grow (Fig.1f,g).

We now consider the evolution of chaotic oscillatory-rotatory attractor P_0 when parameter γ varies. To do so, let us consider bifurcation diagram $\{\gamma,x\}$ given in Fig.2a for σ=0.5, b=10, ε_1=1, ε_2=2, ε_3=3, ε_4=5.75, α=5,

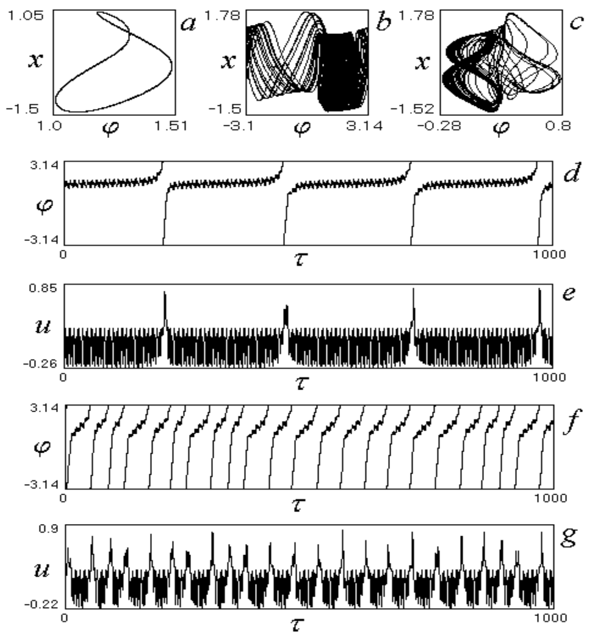

Fig. 1. Phase portraits and time realizations $\varphi(\tau)$ and $u(\tau)$

m=0.1. In Fig.2b (φ,x)-projection of phase portrait and waveform $x(\tau)$ corresponding to attractor P_0 are given. We found that, when γ grows, irregular alternation of

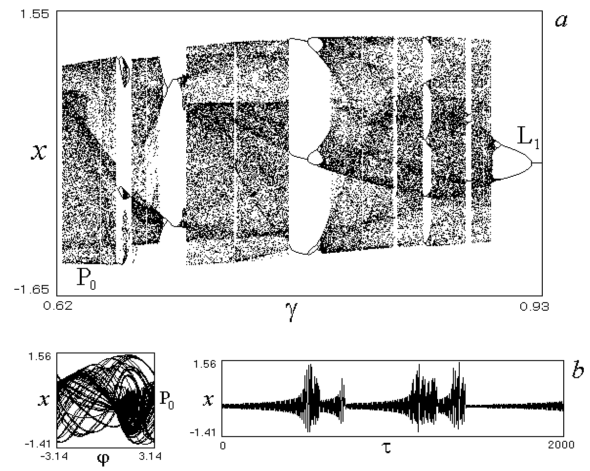

Fig. 2. Bifurcation diagram $\{\gamma,x\}$, phase portrait of attractor P_0, and waveform $x(\tau)$

chaotic and periodic oscillations is observed. Chaotic regimes are formed on the base of rotatory two-turn (4π-periodic by φ), three-turn (6π-periodic by φ), and five-turn (10π-periodic by φ) limit cycles via period-doubling bifurcations. When γ exceeds the value 0.9237 the mode of chaotic attractor is softly transformed to the mode of rotatory one-turn (2π-periodic by φ) limit cycle L_1. With a further increase of γ we observed 2D torus T_1 of rotatory type which is born from limit cycle L_1 when a pair of complex-conjugated cycle L_1 multiplicators crosses the unit circle at γ>0.9437. As γ is increased torus T_1 breaks down and the system enters a mode of rotatory two-turn limit cycle L_2 via chaotization of oscillations. The mode of cycle L_2 exists while γ increases in interval (0.9632,1.3474). A still increase of γ leads to formation of chaotic mode which then replaced by the mode of rotatory five-turn limit cycle L_3. At γ>1.4908 this mode rigidly transformed to the mode of rotatory one-turn limit cycle L_4.

Note that when γ>1.487 stable T_2 and unstable T_3 rotatory 2D torus exists in the phase space simultaneously with limit cycles L_3 and L_4. Fig.3a shows the phase portrait of mapping T_φ of plane $\varphi=\varphi^0$ onto plane $\varphi=\varphi^0+2\pi$ generated by the phase trajectories of system (2). It characterized by the presence of closed invariant curves Γ_1 and Γ_2 corresponding to torus T_2 and T_3, central stable fixed point corresponding to limit cycle L_4, and cycle of five-fold stable fixed points corresponding to limit cycle L_3. Which of the asynchronous modes would be realized in the system it depends on the initial conditions. At γ>1.489 the mode of chaotic attractor appears on the base of torus (Fig.3b). This mode is transformed (Fig.3b-3d) again to the modes of torus T_2 when γ exceeds the value 1.576 (Fig.3e). Then the mode of quasi-periodic oscillation disintegrates and after that the system rigidly switches to the mode of rotatory six-turn (12π-periodic by φ) limit cycle L_5 which is softly transformed to the mode of rotatory three-turn limit cycle L_6. At γ>1.802 the system rigidly switches to the mode of limit cycle L_4.

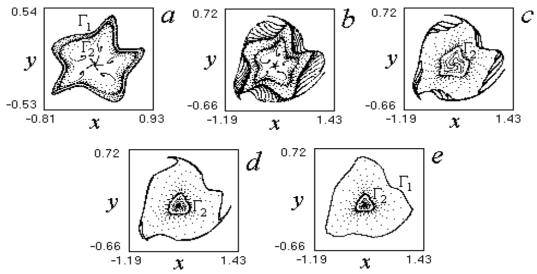

Fig. 3. Evolution of mapping T_φ with increasing of γ

When γ passes through the value γ=1.954, we observe again bifurcation of birth of torus T_2 and T_3, which exist simultaneously with limit cycle L_4. In Fig.4a invariant closed curves Γ_1 and Γ_2 correspond to torus T_2 and T_3, fixed point K corresponds to cycle L_4. At γ>1.976 torus T_2 (curve Γ_1) is destroyed and the phase trajectories converge to rotatory seven-turn (14π-periodic by φ) limit cycle L_5 (Fig.4b). In Fig.4b seven-fold stable fixed points O_1,O_2, …, O_7 correspond to cycle L_5. As γ increases limit cycle L_5 loses its stability with appearance of rotatory seven-turn torus T_4. In Fig.4c cycle of invariant closed curves C_1,C_2, …, C_7 corresponds to torus T_4. Then torus T_4 (curves C_1,C_2, …, C_7) are destroyed and invariant closed curve Γ_1 corresponding to torus T_2 formed from loop of invariant separatrix curves of saddle seven-fold fixed point, invariant closed curves Γ_2 disappears in consequence of reorganization of invariant separatrix curves of saddle seven-fold fixed point. After that the phase portrait of mapping T_φ has the following structure (Fig.4d): curve Γ_1 incorporates cycle of seven-fold fixed points O_1,O_2, …, O_7 became unstable, cycle of saddle seven-fold fixed points, and stable fixed point K.

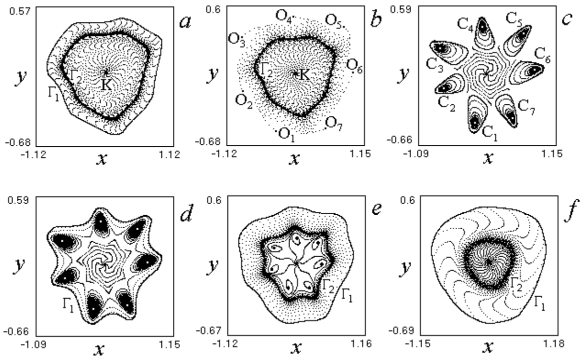

Fig. 4. Evolution of torus T_2 and T_3 with increasing of γ

As γ increases, fixed points $O_1, O_2, \ldots, O_7$ return its stability and unstable invariant closed curve Γ_2 appears again in consequence of reorganization of invariant separatrix curves of saddle seven-fold fixed point (Fig.4e). When passing through the value $\gamma = 2.0111$, seven-fold fixed points disappears due to a saddle-node bifurcation. After this bifurcation stable torus T_2 and unstable torus T_3 exist in the phase space simultaneously with the stable limit cycle L_4 (Fig.4f). Then irregular alternation of mode of torus T_2 and asynchronous mode of rotatory limit cycle is observed, as L_4 increases.

Now we consider asynchronous mode of limit cycle L_4 as the initial state of the system and let us track the evolution of cycle L_4 when γ decreases in the interval (2.0, 0.93). We observe qualitatively another character of the system behavior. When $\gamma < 1.386$, limit cycle L_4 lose its stability via the bifurcation of generation in phase space U of stable 2D rotatory torus T_5. The phase portrait of mapping T_φ (Fig.5a) is characterized by the presence of stable invariant closed curve Γ_3 corresponding to torus T_5 and unstable fixed point K incorporated into Γ_3 and possessing a pair of multiplicators located outside of unit circle. Fixed point K corresponds to limit cycle L_4 that became unstable. When $\gamma < 1.3432$, one of the multiplicators passes the value (–1) and moves interior of the unit circle. As a result of this bifurcation a cycle of two-fold unstable fixed points (K_1, K_2) of mapping T_φ appears (in accordance with [Neimark and Landa, 1987]) that corresponds to unstable two-turn rotatory limit cycle L_6 (Fig.5b).

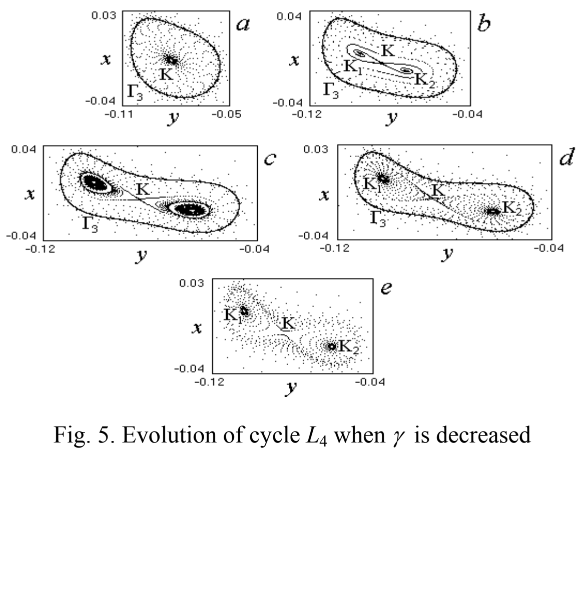

Fig. 5. Evolution of cycle L_4 when γ is decreased

Then for $\gamma < 1.3356$ a bifurcation occurs when the pair of complex-conjugated multiplicators of unstable limit cycle L_6 crosses the boundary of the unit circle moving inwards. As a result of this bifurcation unstable cycle L_6 transforms (in accordance with [Neimark and Landa, 1987]) into stable one; concurrently unstable 2D rotatory two-turn torus T_6 separates from this cycle. Torus T_6 corresponds in the phase portrait of mapping T_φ to invariant closed curves Γ_4 and Γ_5 incorporating stable fixed points K_1 and K_2, respectively, and located within curve Γ_3 (Fig.5c). When γ decreases, curves Γ_4 and Γ_5 merges with the loops of separatrix invariant curves of saddle fixed point K. As a result of this bifurcation unstable 2D rotatory one-turn torus T_7 appears in the phase space. Torus T_7 corresponds to invariant closed curve Γ_6 of mapping T_φ that incorporates fixed points K, K_1, and K_2 ,and locates within the curve Γ_3 (Fig.5d). If γ further decreases, curves Γ_3 and Γ_6 (torus T_5 and T_7) move towards each other and disappear when $\gamma < 1.3321$. As a result of this bifurcation the system rigidly switches from the mode of quasi-periodic asynchronous mode to periodic asynchronous mode of limit cycle L_6 (Fig.5e) which corresponds to stable fixed points K_1 and K_2.

Note that, when $\gamma < 1.295$ one more rotatory two-turn limit cycle L^2 appears as a result of saddle-node bifurcation except limit cycle L_6. When $\gamma < 1.2908$, cycle L^2 became unstable with separating stable rotatory two-turn torus T^2 from this cycle. Fig.6a-6c present (φ, y)- and (φ, x)-projections of phase portraits corresponding to stable limit cycle L^2 and torus T^2, and (y, x)-projection of mapping T_φ corresponding to torus T^2. In Fig.6c invariant closed curves Γ_7 and Γ_8 correspond to torus T^2, fixed point K_3 corresponds to stale limit cycle L_1, and fixed points N_1 and N_2 correspond to limit cycle L^2 that became unstable. As γ decreases, two-turn torus T^2 transforms to one-turn torus T^0 (Fig.6d,e) due to merge of invariant closed curves Γ_7 and Γ_8 with loops of separatrix invariant curves of saddle fixed point K_3. Torus T^0 corresponds to invariant closed curve Γ_9 of mapping T_φ (Fig.6d) and exits in the phase space simultaneously with rotatory two-turn limit cycles L_6 which is stable and B_6 which is a saddle type. When $\gamma < 1.2841$, torus T^0 is destroyed as a result of reorganization of separatrix invariant curves of saddle fixed points of mapping T_φ corresponding to limit cycle B_6. After that the system rigidly switches to the mode of limit cycle L_6.

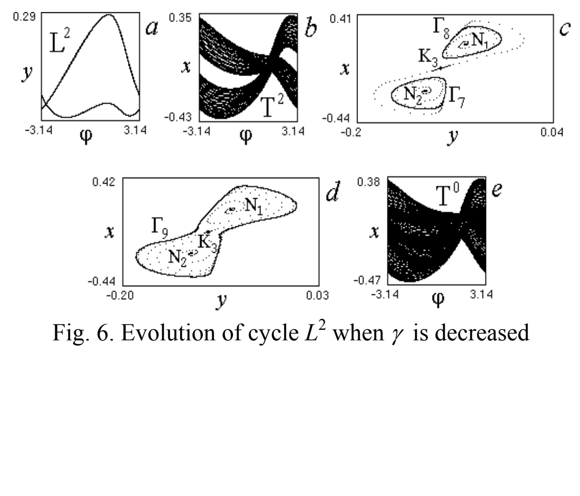

Fig. 6. Evolution of cycle L^2 when γ is decreased

The asynchronous modes of the system that emerge when γ decreases further, are illustrated by bifurcation diagram $\{\gamma, x\}$ given in Fig.7a. It shows how the mode of cycle L_6 is developing while mistuning γ varies from 1.285 to 0.93. In the beginning the mode of cycle L_6 are rigidly replaced by the mode of 2D rotatory one-turn torus T_8 when γ<1.2771. A still decrease of γ leads to appearance at the $\{\gamma,x\}$-diagram of "windows" of stable rotatory limit cycles. Note that, number of rotation by φ corresponding to these limit cycles is diminish two unit worth in succession. The last of these windows corresponds to one-turn limit cycle L_1 for γ<0.9428. Fig.7b shows the fragment of the $\{\gamma,x\}$-diagram in the interval 1.134<γ<1.25. One can distinctly see at this fragment the windows of limit cycles with the number of rotation by φ from 21 to 5. Note that, inside the windows of seven-, five-, and three-turn limit cycles there are realized transitions to chaotic modes via period-doubling bifurcations.

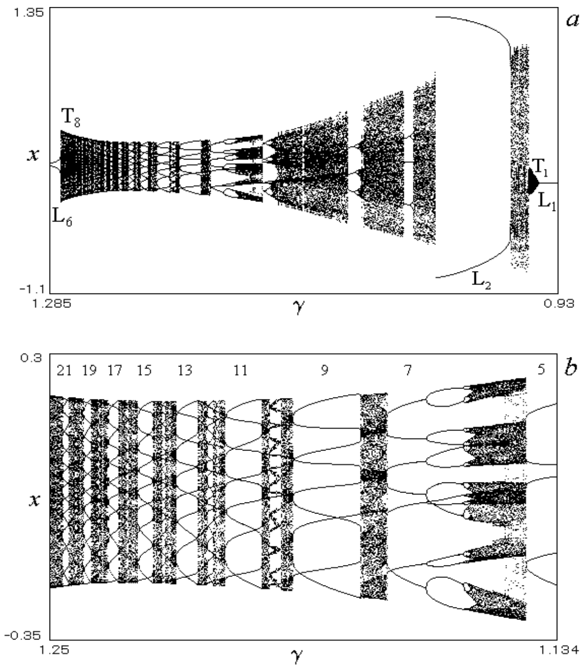

Fig. 7. Evolution of the mode of cycle L_6 with decreasing of γ

The study of mapping φ structure shows that distortion of invariant closed curve corresponds to torus T_8 is observed after the window of fifteen-turn limit cycle. This phenomenon indicates gradual transformation the mode of torus T_8 to the mode of rotatory chaotic attractor. Fig.8 presents the (x,y)-projection of mapping T_φ that shows how the structure of chaotic attractor changes while γ varies in the interval between the windows of fifteen-turn and one-turn limit cycles. At γ<1.0161 the mode of chaotic oscillations is rigidly replaced by the asynchronous mode of two-turn limit cycle L_2. When γ<0.963, limit cycle L_2 vanishes via saddle-node bifurcation and the system transits to the mode of chaotic oscillations via intermittency. As γ is further decreased, this mode is rigidly replaced by the mode of torus T_1 via intermittency chaos-torus type. When γ<0.9428 the mode of torus T_1 undergoes a mild transformation to the mode of limit cycle L_1.

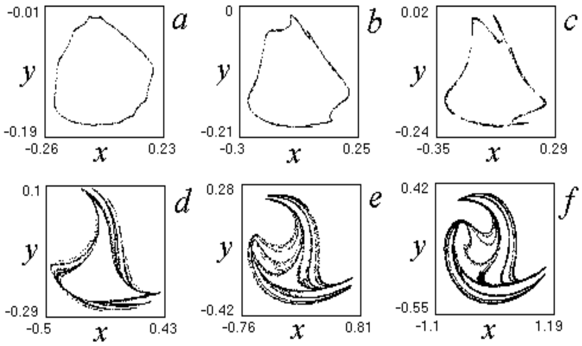

Fig. 8. Evolution of mapping T_φ with decreasing of γ

5 Conclusion

In this paper, we have investigated the dynamical states and bifurcational transitions in coupled systems with phase and delay control in the case when the PLL subsystem is characterized by regular individual dynamics and the DLL subsystem may exhibit both regular and chaotic dynamical modes. We intended to draw the reader's attention to the rich and promising potentialities of the collective dynamics of coupled PLL and DLL subsystems for generation of complex oscillations the properties of which can be controlled by means of parameters of the system. Within the framework of five-dimensional dynamical model conditions of synchronous mode stability are obtained in the form of requirements (4), and the system behavior are studied when parameter values live the synchronous mode stability domain. It is found that the coupled PLL and DLL demonstrate a rich variety of dynamical states and bifurcations when initial frequency mistuning γ varies. The considered model illustrates typical scenarios of transition to chaos, principal types of attractors and its bifurcations. The dynamical phenomena in model (2) are of fundamental importance for understanding the behavior of coupled PLL and DLL when it is brought into a regime of synchronization and when the synchronous mode is cut off as a result of the perturbation of phase variables and system parameters. The results of our analysis of the considered model dynamics allow to make a conclusion that the system of coupled PLL and DLL may be regarded as a generator of chaotically modulated oscillations.

Acknowledgments

This study was supported by the Russian Foundation for Basic Research (grants No 05-02-17409, No 06-02-16499).

References

Tuzov, G.I., Sivov, V.A., Prytkov, V.I., et al., Pomekhozashchishchennost' radiosistem so slozhnymi signalami (Noise Protection of Radio Systems with Com-

Complex Signals), Tuzov, G.I., Ed., Moscow: Radio i Svyaz', 1985.

Babich, O.A. Obrabotka informatsii v navigatsionnykh kompleksakh (Processing of Information in Navigation Complexes), Moscow: Mashinostroenie, 1991.

Ponomarenko, V.P., Izvesiya VUZ. Applied Nonlinear Dynamics (Saratov), 2002, vol. 10, no. 1-2, p. 65.

Neimark, Yu.l. and Landa, P.S., Stokhasticheskie i khaoticheskie kolebaniya (Stochastic and Chaotic Oscillations) Moscow: Nauka, 1987.